DOI: 10.13009/EUCASS2023-644
Aerospace Europe Conference 2023 – 10TH EUCASS – 9TH CEAS

Design of translunar injection trajectories using phasing loops in a TPBVP

Fu-Yuen Hsiao[⋆†] *and Chun-Wai Wong*[⋆]
[⋆]*Department of Aerospace Engineering, Tamkang University*
151 Ying-zhuan Rd., Tamsui, New Taipei 25137, TAIWAN
fyhsiao@mail.tku.edu.tw · ben9206wong@gmail.com
[†]Corresponding author

Abstract

This paper studies the design process of translunar injection (LTI) trajectories using phasing loops given initial and terminal conditions. Starting from the two-body problem (2BP) assumption, a highly perturbed restricted three-body problem (ER3BP) environment is eventually introduced in the investigation of the algorithms. Exploring the moon becomes a worldwide space mission recently, owing to the potential of human inhabitant. The Taiwan Space Agency (TASA), formerly known as NSPO, initiated a preliminary study on the lunar exploration in 2019. Although low energy transfers, such as ballistic lunar transfer, are more and more welcome nowadays, translunar injection using phasing loops is still a safer and easier choice for an inexperienced space agency. This paper, as an extended work of,[1] intends to develop a generic design process applicable to an arbitrarily given initial and final conditions. In specific, this problem can be formulated as a two-point boundary value problem (TPBVP) whose conditions include initial time, initial position of the lunar probe, arrival time, and desired final position. There are two major contributions achieved in this paper. In[1] the probe only aims roughly at the moon, in this paper, however, a more specific location is targeted. Moreover, the influence of the resolution of the probe thruster is also analyzed. The 2BP assumption is initially employed to determine coarse parameters. Then an algorithm of iterations is proposed to correct the trajectory subject to major perturbations, such as J2, lunar gravity and solar gravity, etc. In order to tune the parameters more efficiently, the ER3BP environment and Lambert?s theorem are also introduced in the process. The Systems Tool Kit (STK) is also used to simulate the trajectory with the found parameters under the fully perturbed environment. The developed algorithm in this paper is potentially applicable to various lunar mission scenarios using phasing-loop transfer provided desired initial and terminal conditions.

1. Introduction

This research project intends to develop an algorithm that designs the translunar injection (TLI) trajectory in the environment of elliptic restricted three-body problem (ER3BP), as an extension of our previous studies on Taiwan's lunar mission supported by the Taiwan Space Agency (TASA), formerly known as the National Space Organization (NSPO) before 2023, and National Science and Technology Council (NSTC). Although an outer space exploration with our own spacecraft is temporarily halted by the TASA recently, it might be one of the choices in the near future. Some preliminary studies has be done under the support of NSPO and NSTC. These studies will be briefed later.

Choi et al. (2016) analyzed a visibility condition of KPLO based on the combination of various candidate ground stations and the masking angles by utilizing 3.5 phasing options. In addition, the optimum satellite-Earth-Moon (SEM) angle is suggested in Choi et al. (2018a) from a number of viewpoints including launch epoch, coast duration, perigee altitude, and delta- Vs, regarding not only the transfer but also LOA phases as the SEM angle defined in the Earth-Moon rotating frame is a critical constraint in evaluating the 3.5 phasing loop transfer trajectory. Choi et al. (2018) recently conducted a number of trade-off studies of KPLO transfer options to minimize the delta-V, including phasing loop options, translunar inclinations, and 1st apogee altitude.[2–6] Lee et al. (2017) examined the effect of steering angle constraint during finite burn maneuvers to optimize fuel usage during a finite burn.[7] For effective station-keeping, Park et al. (2018) recently proposed an enhanced control technique to reduce delta-V costs for the KPLO mission and demonstrated it by comparing it to algorithms implemented in previous lunar reconnaissance orbiter (LRO) and KAGUYA missions.[8]

DOI: 10.13009/EUCASS2023-644

Some excellent work regarding the dynamics of ER3BP are presented in.[9–12] Szebehely's work is one of the very early achievement on ER3BP[9] . Unlike other work regarding ER3BPs which usually approached the problems in true anomaly, investigation by Umar and Hussain extend the current work of ER3BP in the space of eccentric and proposed a very neat form of Jacobi integrals.[10,11] Umar and Hussain also integrated some perturbations in the force potential. Miller investigates the methods to design TLI using ER3BP[12] .

This research is a continuing work of our previous investigation on the design of TLI trajectory. In our previous study,[1] where we proposed a design procedure for any given boundary conditions, and approached this problem under the two-body problem and CR3BP, respectively. We also did some preliminary study on how to design a trajectory under ER3BP. Then J_2 effect is added as perturbations. With the found parameters, GMAT and STK are employed for the final modifications of parameters. However, in the simulation the spacecraft never arrives in the targeted location is due to the strong lunar gravitational perturbation. In this work we approach this problem with the employment of the ER3BP assumption systematically, especially when the spacecraft arrives in the vicinity of the moon. It is difficult to reach the target point without any deviation by just changing the initial conditions and design of different phasing loops without making any correction maneuvers. Therefore, we use Lambert's theorem to design maneuvers to correct to the target point, and analyze the optimal timing for the correction. In addition, we use differential correction based on a linear system to find the optimal initial conditions to achieve the purpose of trajectory optimization.

2. Problem Formulation and Specifications

2.1 Translunar Injection with Phasing Loops

Currently in orbital design, there are many different methods of orbital transfer, such as Hohmann Transfer, Bi-Elliptic Transfer, Geostationary Transfer Orbit, Phasing Loop Transfer, and so on. Phasing loops are composed of ellipses with different semi-major axis (SMA) lengths. There are actually two cases, one is acceleration, the other is deceleration. When the situation involves satellite acceleration, the sequence of elliptical orbits goes from a smaller semi-major axis to a larger one. There is no limit to the number of elliptical orbits in between, but the transition goes from an inner elliptical orbit to an outer one. The procedures for deceleration is just the opposite. An example is shown in Fig. 1.

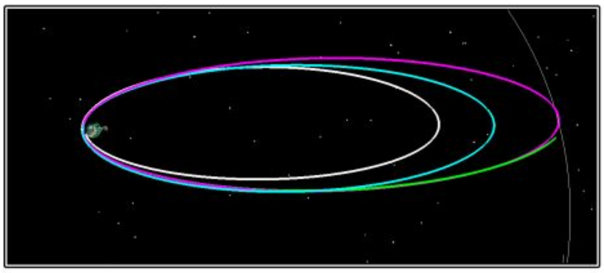

Figure 1: Translunar injection trajectory of LADEE mission[13]

Phasing loop transfers offer significant flexibility in trajectory design. Consider a satellite bound by a maximum propulsion maneuver of 0.25 km/s at each instance. Utilizing a Hohmann transfer may demand a ΔV exceeding the 0.25 km/s threshold, presenting a challenging scenario. This issue can be circumvented by employing phasing loops, although this method requires a longer overall duration.

The extended time of flight with phasing loops confers several benefits. Firstly, it offers ample opportunity for correcting potential maneuver errors. Secondly, it provides more leeway to ensure the mission adheres to the desired arrival time. However, a notable disadvantage of a longer flight time is the extended exposure to various perturbations such as air drag and gravitational perturbations from the Earth and the Sun. As such, correction maneuvers are essential when adopting phasing loop transfers. Compared to other strategies, phasing loops are more forgiving and offer the ability to execute maneuvers in response to various issues, thus lowering the entry barriers for designing a deep-space trajectory, particularly for less experienced space agencies.

Phasing loop transfers are flexible in designing a transferring trajectory. Suppose a satellite is constrained with a maximum propulsion maneuver of 0.25 km/s each time. Hohmann transfer may require a ΔV exceeding 0.25 km/s. This problem can be solved by using phasing loops, but the entire process will take a longer time with phasing loops. The advantages of longer time of flight is that there is more space to correct potential maneuver errors and more freedom to satisfy arrival time. The drawback is that the duration under perturbations like air drag or gravitational perturbations from earth and sun is longer. Hence, correction maneuvers are necessary when employing phasing loop transfers.

DOI: 10.13009/EUCASS2023-644

Compared to other methods, the phasing loop has a higher tolerance, and maneuvers can be made in response to different problems, providing lower threshold in designing a deep space trajectory for an unexperienced space agency.

2.2 Specifications in TASA's Preliminary Studies

In 2019, TASA embarked on a preliminary study focusing on lunar exploration. Given their limited experience in deep space exploration, TASA intended to incorporate phasing loops for TLI trajectories. Additionally, in consideration of spacecraft manufacturing capabilities, TASA stipulated the following specifications for trajectory design:

1. Specifications of lunar orbiter:
   (a) Dry mass: 150 kg
   (b) Isp of the orbiter thruster $\geq$ 200 s
2. Specifications of trajectory design:
   (a) Parking orbit
      i. Type: Geostationary transfer orbit (GTO)
      ii. Altitude of orbit: 500 km $\times$ 3600 km
      iii. Inclination: Coplanar to the orbit of the moon
   (b) Mission Orbit about Moon:
      i. Altitude of orbit: 100 km $\times$ 100 km
      ii. Inclination: 90°
      iii. Mission duration $\geq$ 1 year
   (c) Trans-lunar injection Trajectory: Phasing Loop Transfer
      i. Time of flight $\leq$ 9 weeks
      ii. Maximum maneuver each time: $\Delta v_{max} \leq 0.3$ km/s

Although the design of lunar orbit was included in the study, this paper only discuss the design of TLI trajectory. Moreover, we assume the initial and terminal time on our own when studying this problem, since it is very difficult to approach the the results with open mission duration. In this following list our assumption.

- Departing time: T_{start} =10 Sep 2023 00:00:00.000 UTC
- Arrival time: T_{arrive} = 08 Oct 2023 16:00:00.000 UTC

According to the assumption, time of flight (TOF) can be found by $T_{tf} = T_{arrive} - T_{start} = 2476800.000287$ (s). Because the initial and arrival times are defined. The terminal states are also defined, since the location of moon can be predicted with the arrival time. This converts the problem to a two-point boundary value problem (TPBVP) with fixed terminal time.

3. Preliminary Approach in Two-Body Problem

3.1 Problem Formulation

The preliminary approach is studied under the two-body problem (2BP) assumption, as detailed in Wong's work.[1] In addition to the assumptions mentioned in the preceding sections, we impose two more constraints on the problem. Firstly, maneuvers that change loops always occur at the perigee. Secondly, the spacecraft is initially placed at a location with a true anomaly of f_0, a presumption made without loss of generality. The application of the second assumption results in an additional time T_{i2p} for the spacecraft to reach the perigee at the outset. This also makes the allowable transferring for phasing loops become $T_{phasing} = T_{tof} - T_{i2p}$. The minimum loops of TLI trajectory in our case is 3.5 loops.[1]

Assume the spacecraft is initially placed in a parking orbit, referred to as A0. After a certain number of loops, a thrust Δv_1 is applied at the perigee to transfer the spacecraft to the A1 loop. Similarly, after completing several loops in A1, a thrust Δv_2 is applied at the perigee to move the spacecraft to the A2 loop. Subsequently, a thrust Δv_3 is employed

DOI: 10.13009/EUCASS2023-644

to facilitate a transfer to the A3 loop. In this scenario, the Moon is assumed to be located at the apogee of A3. As a result, only half of the A3 loop is utilized in the flight path. Hence, we conclude

$$T_{tf} = T_{i2p} + n_0 T_0 + n_1 T_1 + n_2 T_2 + \frac{1}{2} T_3 \tag{1}$$

where T_k, $k = 1, 2, 3$ are the periods of each loop and n_k are the number of loops.

3.2 Algorithm to Determine Loops

According to the assumptions, the following algorithm is developed:

1. Assume that T_{i2p} and n_0 are known or given. Since T_{i2p} depends on the location where the spacecraft is released from a rocket and n_0 depends on the time required for the spacecraft to do health check on the parking orbit before her trip to the moon, they are predefined by the mission. Moreover, the final loop, denoted by subscript 3, is determined by the perigee and the radius of the moon, the period is fixed. Hence, it is concluded that

$$\Delta t_{1,2} \quad = \quad T_{tf} - T_{i2p} - n_0 T_0 - \frac{T3}{2} \tag{2}$$

2. The identified Δt is evenly distributed between the phasing loop orbits A_1 and A_2.

$$T_{PL,a_1} \quad = \quad T_{PL,a_2} = \frac{\Delta t_{1,2}}{2} \tag{3}$$

3. Assume that both $\Delta v1$ and $\Delta v2$ are the maximum maneuvers, from which we can find the applicable semi-major axis a_k and its corresponded period T_k, where $k = 1, 2$.

4. The number of loops in each phasing can be found by $\frac{\Delta t}{T}$, which identifies the permissible number of loops. However, since the number of loops must be an integer, the suitable semi-major axis length and its loop number can be found by adjusting n_1 and n_2.

$$n_k \quad \leq \quad \frac{\Delta T_k}{T_k}, n_k \in N; \quad k = 1, 2 \tag{4}$$

5. Introduce a new parameter δn_1 for the phasing loop A1 orbit to adjust the value of n_1, so as to provide more choices for n_2 and a_2, thus increasing the flexibility of adjustments.

6. Since the thrust cannot exceed Δv_{max}, it is concluded that $\Delta v_{2_{min}} \leq \Delta v_2 \leq \Delta v_{2_{max}}$, where $\Delta v_{2_{min}}$ can be found by assuming Δv_1 and Δv_3 are maximum. Wong's work approximates the total Δv_{tf},[1] and $\Delta v_{2_{min}}$ is given by Eq. (5).

$$\Delta v_{2_{min}} \quad = \quad \Delta v_{tf} - 2\Delta v_{max} \tag{5}$$

   The corresponded semi-major axis of A2 after Δv_2 is applied can be found, which satisfies $a_{2_{min}} \leq a_2 \leq a_{2_{max}}$.

7. Using the results obtained from Step 5, plot the relationship between a_2, the orbital period time, and the number of loops.

8. Select suitable values for n_1, a_2, and n_2, so that the error of $\Delta t_{1,2} - (n_1 T_1 + n_2 T_2)$ is minimized.

9. Use the selected a_2 and n_2 in the previous step to find the Δv_2 that allows the satellite to transfer from A1 orbit to A2 orbit.

10. Determine A3 by compute $\Delta v_3 = \Delta v_{tf} - \Delta v_1 - \Delta v_2$.

3.3 Example Mission and Numerical Simulations

An example mission is devised to illustrate the robustness of the proposed algorithm. In addition to the specifications provided by TASA, the initial orbital elements of the spacecraft are assumed for this demonstration mission. Table 1 presents the orbital elements of the spacecraft at the point of departure and the Moon's orbital elements at the time of arrival.

The design results from the proposed algorithm are presented in Table 2, and the resulting trajectory is presented in Fig. 2. By examining the final states we conclude that no errors exist between the terminal location of the spacecraft and the moon.

DOI: 10.13009/EUCASS2023-644

Table 1: orbital elements of the spacecraft at the point of departure and the Moon's orbital elements at the time of arrival

O. E.	Moon (Arrival)	Spacecraft (Departure)
a	386467.0734 (km)	24628.1370 (km)
e	0.0522	0.7207
i	28.1881 (deg)	28.1881 (deg)
Ω	4.6765 (deg)	4.6765 (deg)
ω	-40.0787 (deg)	298.9982 (deg)
f	159.07683 (deg)	167.8475 (deg

Table 2: Final selected Δv, semi-major axis, and loops at each phase.

	Δv_k (km/s)	a_k (km)	T_k (sec)	n_k (loops)
Parking	/	24628	38464.3646	5
Phasing A1	0.3000	39452.9088	77988.3559	10
Phasing A2	0.1649	59640.3488	144951.0888	7
Phasing A3	0.2248	206034.7286	930726.0425	0.5

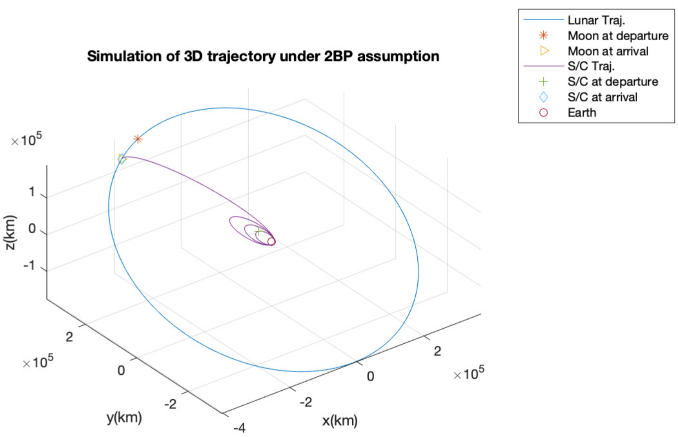

Figure 2: Complete TLI trajectory designed with the proposed algorithm in the 2BP environment.

DOI: 10.13009/EUCASS2023-644

4. Perturbations and Solutions

While the proposed algorithm performs well in a two-body problem (2BP) environment, numerous perturbations exist in the real world. These include atmospheric drag, the Earth's J_2 (second zonal harmonic) effect, gravitational pull from the Earth, Sun, Moon, and other planets, solar wind, solar radiation pressure, and so forth. In this preliminary study, we only take into account the major perturbations, including the Earth's J_2 effect, the gravitational pull from the Sun, and the gravitational pull from the Moon. However, due to the specific characteristics of the trajectory, these perturbations are not all considered simultaneously. When the spacecraft is near Earth, the J_2 effect is factored in. In the A3 loops, which guide the spacecraft, we consider the effect of solar gravitation. As the spacecraft nears the Moon, the trajectory is fully simulated numerically, with all considered perturbations factored in.

4.1 J_2 Effect and Solution

The J_2 effect arises from the Earth's equatorial bulge, which results in an uneven distribution of gravitational forces. Because gravitational pull is inversely proportional to the square of the distance, the J_2 effect diminishes rapidly as the spacecraft moves farther from Earth. As such, the J_2 effect is only considered when the spacecraft is in proximity to Earth, specifically during the A0, A1, and A2 loops.

Under the J_2 effect, averaged eccentricity and inclination keep constant. Averaged longitude of ascending node, argument of periapsis and semi-major axis vary with time. The variation of semi-major axis results in the variation of averaged period time. Hence, the time for the spacecraft to be in the periapsis changes significantly after several loops.

We first numerically integrate the trajectory with J_2 effect for several orbit periods. The orbit period is defined in the 2BP environment, i.e., $T = 2\pi\sqrt{a^3/\mu_e}$, where μ_e is the gravitational parameter of the Earth. Due to the J_2 effect, the spacecraft won't arrive in the perigee at the end of integration, meaning that $M \neq 2n\pi$. With this operation we are able to obtain the average change rate of mean anomaly in each phasing by

$$\dot{M}_k = \frac{M_{k,test}}{n_{k,test}T_k} \tag{6}$$

where n_k is the integrated number of orbits in the A_k phasing. Then, when we first simulate n_k loops for the A_k phasing, we may get mean anomaly M_k at the end of simulation. As a result, the time Δt_k to correct will be

$$\Delta t_k = \frac{2n_k\pi}{\dot{M}_k} - n_k T_k \tag{7}$$

Considering the correction of time, Eq (8) is obtained.

$$T = T_{i2p} + \sum_{k=1}^{3}(n_k T_k + \Delta t_k) \tag{8}$$

4.2 Trajectory near the Moon

In the 2BP simulations, the spacecraft is aimed at the center of the moon, without considering lunar gravitation. However, this is unrealistic in actual missions. According to the specifications provided by TASA, the spacecraft is intended to orbit the moon at an altitude of 100 km. Moreover, the gravitational perturbations are quite complex in the vicinity of the moon. Due to the uneven distribution of the moon's mass, its gravitational field is intricate. On the other hand, the moon's mass is relatively small compared to that of the Earth or the Sun. This means that the gravitational influences from both the Sun and the Earth also play a substantial role in the spacecraft's trajectory near the moon.

To address these complexities, we utilize STK (Systems Tool Kit) for simulation, which takes into account full perturbations. For the lunar orbit insertion (LOI), the patched conic approximation method is used to determine the spacecraft's state at the moon's sphere of influence (SOI). Furthermore, to find the phasing for A3, we apply the back-propagation algorithm.

In our trial, we first select a potential periluna. Then, we apply the back-propagation algorithm to find the required states of the spacecraft, specifically the position and velocity, in the Sphere of Influence (SOI) of the Moon with full perturbations in the STK simulator . The SOI is a sphere centered on the Moon, with a radius r_{SOI}, which is estimated by:

$$r_{SOI} = a_m\left(\frac{M_m}{M_e}\right)^{0.4} \tag{9}$$

DOI: 10.13009/EUCASS2023-644

where a_m is the semi-major axis of the lunar orbit, M_e is the mass of the Earth, and M_m is the mass of the moon. The time of flight to integrate backward is approximated under 2PB assumption.

Four examples are provided in Figs 3. In these examples, all other parameters are identical but the longitude of ascending node Ω. Consequently, the final states of the spacecraft are different.

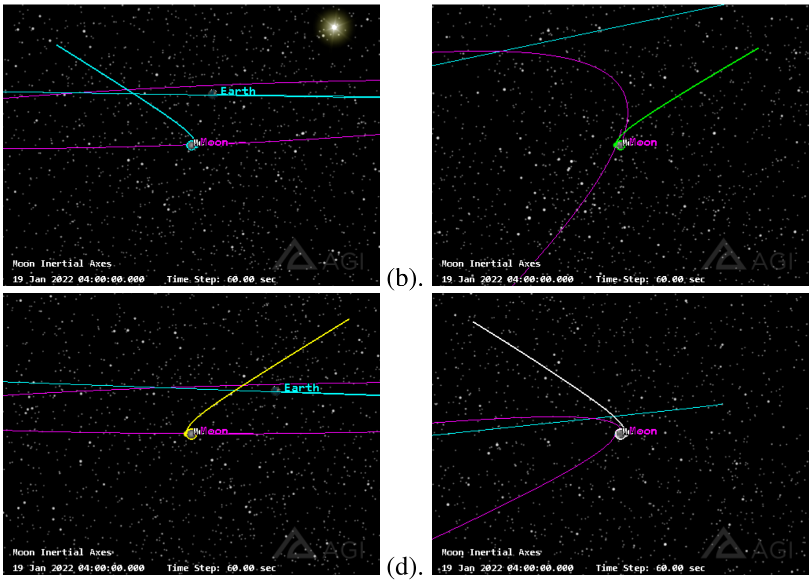

Figure 3: Examples of potential LOI design. (a). $\Omega = 50°$; (b). $\Omega = 140°$; (c). $\Omega = 230°$; (d). $\Omega = 320°$

4.3 Patched-Conic Method

In this study, we use the patched conic approximation method to simplify the problem in the final transfer to the Moon in the last 3.5 phasing loops and find a more suitable orbit insertion trajectory.

In the Earth-Moon boundary, we can simplify the analysis of the multi-body problem by using the patched conic approximation method.[14] As shown in Fig. 4, a trajectory can be divided into two parts. One part is influenced by the gravity of the Earth and the other part, after entering the gravity sphere of influence of the Moon, is affected by the Moon's gravity. Therefore, we can consider the trajectory's states under these two separate gravitational influences. By this method, we can simply split the problem into the Earth's part and the Moon's part for trajectory variation analysis.

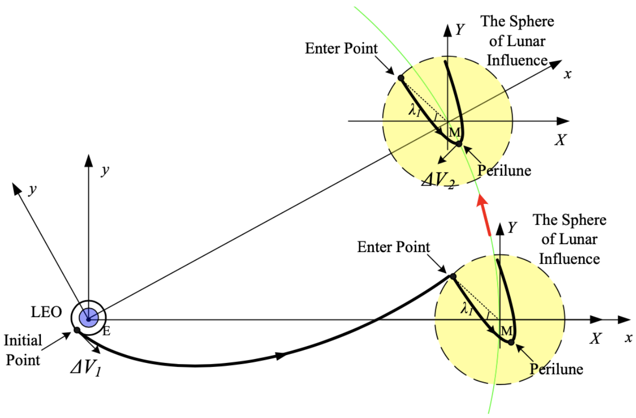

Figure 4: Patched-Conic Method[14] in the Earth-Moon transferring problem.

$$\mathbf{v}_{sc/e} = \mathbf{v}_{sc/m} + \mathbf{v}_m \tag{10}$$

DOI: 10.13009/EUCASS2023-644

where the slash in the subscript denotes "relative to". The velocity within the SOI, as determined by the back-propagation algorithm, is considered relative to the Moon. For further application in the last phasing loop, we need to determine the velocity relative to the Earth, which can be found using Eq. (10).

5. Back-Propagation Algorithm with ER3BP

In the final phasing, the spacecraft traverses from the perigee to the insertion point in the Moon's sphere of influence (SOI), as illustrated in Fig. 4. The majority of this journey takes place under the influence of the Earth's gravity. The effect of the Earth's J_2 can be disregarded as the spacecraft does not remain close to the Earth for an extended period. The gravitational anomaly of the Moon is also negligible as our target is the insertion point on the Moon's SOI, rather than a low lunar orbit.

It is very difficult to design a trajectory that connects the perigee of A2 phasing and the insertion point with the desired states, because the journey is too long and the gravitational environment is too complex, we choose to integrate the trajectory backward from the insertion point under the ER3BP model. Then, try to design another "connecting" trajectory to connect the perigee and the A3 trajectory.

5.1 Elliptic Restricted Three Body Problem

In the ER3BP model, the second primary orbits the first primary in an elliptic orbit, Hence, the orbit angular rate is no longer constant. In the problem we are investigating, the first primary is the Earth and the second primary is the Moon. The equations of motion (EOMs) of the spacecraft are given by[15]

$$\ddot{x} = 2\dot{\theta}\dot{y} + \ddot{\theta}y + \dot{\theta}^2 x - (1-\mu)\frac{(x+\mu R)}{r_1^3} - \mu\frac{(x-(1-\mu)R)}{r_2^3} \tag{11}$$

$$\ddot{y} = -2\dot{\theta}\dot{x} - \ddot{\theta}x + \dot{\theta}^2 y - (1-\mu)\frac{y}{r_1^3} - \mu\frac{y}{r_2^3} \tag{12}$$

$$\ddot{z} = -(1-\mu)\frac{z}{r_1^3} - \mu\frac{z}{r_2^3} \tag{13}$$

where $r_1 = \sqrt{((x+\mu)^2 + y^2 + z^2)}$, $r_2 = \sqrt{((x-1+\mu)^2 + y^2 + z^2)}$ and θ is a parameter in the polar coordinate system. Given f the true anomaly, $\theta = f + \theta_0$, where θ_0 is a constant and $\dot{\theta} = \dot{f}$

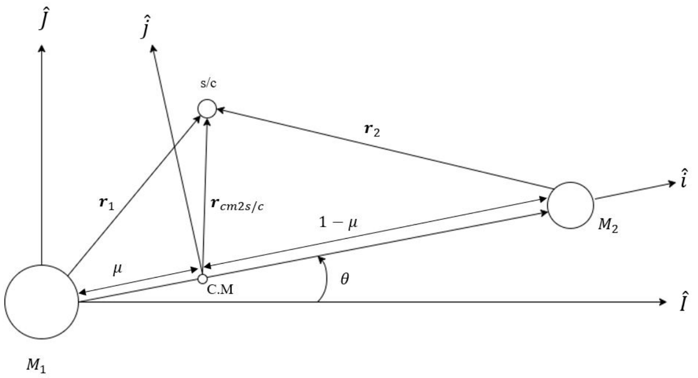

Figure 5: The the Earth-Moon-Spacecraft system in the rotational frame

5.1.1 Change of Domain

Equation (13) in our model represents the three-body problem in the time domain. However, for more comprehensive analysis, problem simplification, and variable reduction, we can convert the original time-domain equation into the true anomaly domain. The rate of change of the true anomaly can be found by differentiating Equation (14) with respect to time. This variable plays a crucial role in both the computation and derivation process. The rate of change of the true anomaly is given by Eq. (15).

$$r = \frac{a(1-e^2)}{(1+e\cos f)} \tag{14}$$

DOI: 10.13009/EUCASS2023-644

$$\frac{d}{dt}r = \sqrt{\frac{\mu}{a^3(1-e^2)^3}}(1+e\cos f)^2 \tag{15}$$

After several manipulations, we are able to obtain the EOMs in the true anomaly domain:

$$\begin{aligned}
\frac{d^2x}{df^2} &= 2\frac{dy}{df} + \frac{1}{1+e\cos f}(x-(1-\mu)\frac{x+\mu}{r_1^3} - \mu\frac{x-1+\mu}{r_2^3}) \\
\frac{d^2y}{df^2} &= -2\frac{dx}{df} + \frac{1}{1+e\cos f}(y-(1-\mu)\frac{y}{r_1^3} - \mu\frac{y}{r_2^3}) \\
\frac{d^2z}{df^2} &= -z + \frac{1}{1+e\cos f}(z-(1-\mu)\frac{z}{r_1^3} - \mu\frac{z}{r_2^3})
\end{aligned} \tag{16}$$

The virtual force potential U in ER3BP is given by[9]

$$U = \frac{1}{1+e\cos f}\left(\frac{1}{2}(x^2+y^2+z^2) - \frac{1-\mu}{r_1} - \frac{\mu}{r_2}\right) \tag{17}$$

Hence, the EOMs can be expressed as the conventional simplified form:

$$\begin{aligned}
x'' - 2y' &= U_x \\
y'' + 2x' &= U_y \\
z'' + z &= U_z
\end{aligned} \tag{18}$$

The Jacobi Integral in the ER3BP can then be defined by

$$\begin{aligned}
C_J &= 2U - (x'^2 + y'^2 + z'^2 + z^2) \\
&= \frac{1}{1+e\cos f}\left(x^2+y^2+z^2+2\frac{1-\mu}{r_1}+2\frac{\mu}{r_2}\right) - (\dot{x}^2+\dot{y}^2+\dot{z}^2+z^2)
\end{aligned} \tag{19}$$

5.1.2 Change of Coordinate Systems

In the A0 to A2 Phasing, the trajectories of the spacecraft are integrated in a Cartesian coordinate system in the inertial frame. The states of the insertion point on lunar SOI are also represented in the same coordinate system. However, the ER3BP should be performed in Cartesian coordinate system in the rotational frame. Hence, the transformation should be derived for the two coordinate system.

Firstly, we identify the states of the spacecraft and the moon under the Earth's inertial frame, and then transform from the original inertial frame to a rotating frame. In this rotating frame, $\boldsymbol{\rho} sc$ and $\dot{\boldsymbol{\rho}} sc$ represent the position and velocity vectors of the spacecraft, respectively.

$$\boldsymbol{\rho}_{sc} = \mathbf{r}_{sc} \tag{20}$$

$$\dot{\boldsymbol{\rho}}_{sc} = \dot{\mathbf{r}}_{sc} + \boldsymbol{\Omega}_{sys} \times \boldsymbol{\rho}_{sc} \tag{21}$$

Then we change the time domain to the true anomaly domain.

$$\boldsymbol{\rho}_t = r \cdot \boldsymbol{\rho}_f \tag{22}$$

$$\frac{d}{dt}\boldsymbol{\rho}_t = \frac{d}{df}(r\cdot\boldsymbol{\rho}_f)\frac{df}{dt} \tag{23}$$

$$r = p/g = \frac{a(1-e^2)}{1+e\cos f} \tag{24}$$

At last the transformation of coordinate systems can be obtained. Define

$$\alpha = \Omega_m \tag{25}$$

$$\beta = ß_m \tag{26}$$

$$\gamma = u = \omega_m + f_m \tag{27}$$

DOI: 10.13009/EUCASS2023-644

The transformation matrix can be found by

$$Q_{I2R} = R_z(-\gamma)R_x(-\beta)R_z(-\alpha) \tag{28}$$

$$Q_{R2I} = R_z(\alpha)R_x(\beta)R_z(\gamma) \tag{29}$$

$$\dot{R}_z = \dot{f}\begin{bmatrix} -\sin(u_m) & -\cos(u_m) & 0 \\ \cos(u_m) & -\sin(u_m) & 0 \\ 0 & 0 & 0 \end{bmatrix} \tag{30}$$

$$\boldsymbol{\rho}_R = R_{I2R}\boldsymbol{\rho}_I \tag{31}$$

$$\dot{\boldsymbol{\rho}}_R = R_{I2R}\dot{\boldsymbol{\rho}}_I + \dot{R}_{I2R}\boldsymbol{\rho}_I \tag{32}$$

Here, Q_{I2R} is the rotation matrix that transitions from the inertial coordinate system to the rotating coordinate system shown in Fig. 5, while Q_{R2I} is the rotation matrix that transitions from the rotating coordinate system back to the inertial coordinate system. $\boldsymbol{\rho}R$ and $\dot{\boldsymbol{\rho}}R$ represent the position vector and velocity vector under the true anomaly domain, relative to the coordinate system shown in Fig. 5. Morever, we still need to move the whole coordinate system to the center of the mass, given by

$$\boldsymbol{\rho}_{R,2cm} = \boldsymbol{\rho}_R - [\mu \quad 0 \quad 0]^T \tag{33}$$

$$\dot{\boldsymbol{\rho}}_{R,2cm} = \dot{\boldsymbol{\rho}}_R \tag{34}$$

5.2 Application of ER3BP

As mentioned earlier, It is very difficult to design a trajectory that connects the perigee of A2 phasing and the insertion point with the desired states, because the journey is too long and the gravitational environment is too complex, we choose to integrate the trajectory backward from the insertion point under the ER3BP model.

In Section 4.3, we select different periluna points. Then, we apply the back-propagation algorithm to find the required states of the spacecraft, specifically the position and velocity, in the SOI of the Moon with the STK simulator, as examples shown in Figs 3. These potential insertion points are further integrated backward using the ER3BP model to obtain the closest points near the Earth. We realized that most of them will be very far away from the perigee of $A2$ phasing. By trials-and-errors method, we may find an insertion point that is resulted from the location near to the the perigee of $A2$ phasing.

6. Lambert's Theorm

The last step to accomplish the design mission is to apply the Lambert Theorem to connect the perigee of $A2$ phasing to the closest point of the the A3 phasing by back-propagation algorithm.

6.1 Equations of Lambert's Theorem

The Lambert problem can be defined as finding a Keplerian orbit about a given gravitational center within a specified time Δt, connecting two given points $P1$ and $P2$, as illustrated in Fig. 6.[16] where, $P1$ and $P2$ can be defined as the departure and arrival points, respectively. These two points can be any point on two individual orbits. By finding the elliptical orbit that connects these two position points, and imposing some time constraints, we can calculate the trajectory of the transition, as illustrated in Fig. 7.

After identifying the orbit connected to these two points, we can proceed using the following two constraints:

$$t_f < t_m \tag{35}$$

$$t_f > t_m \tag{36}$$

To choose the elliptical transition orbit found using Lambert's theorem, we can decide whether to use a longer transition trajectory or a shorter one. This can be determined by the transition time Δt which defines the respective path, as expressed in Eq. (37).

$$\Delta t = \sqrt{\frac{a^3}{\mu}}(\alpha - \beta - (\sin\alpha - \sin\beta)) \tag{37}$$

DOI: 10.13009/EUCASS2023-644

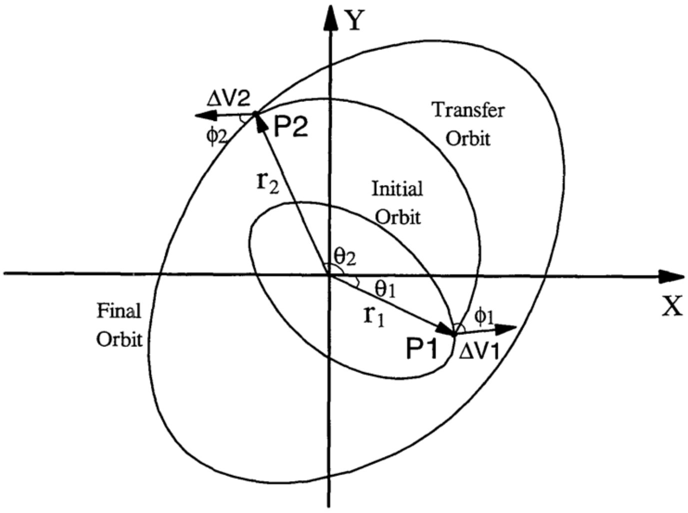

Figure 6: Orbit transformation by Lambert's Theorem[16]

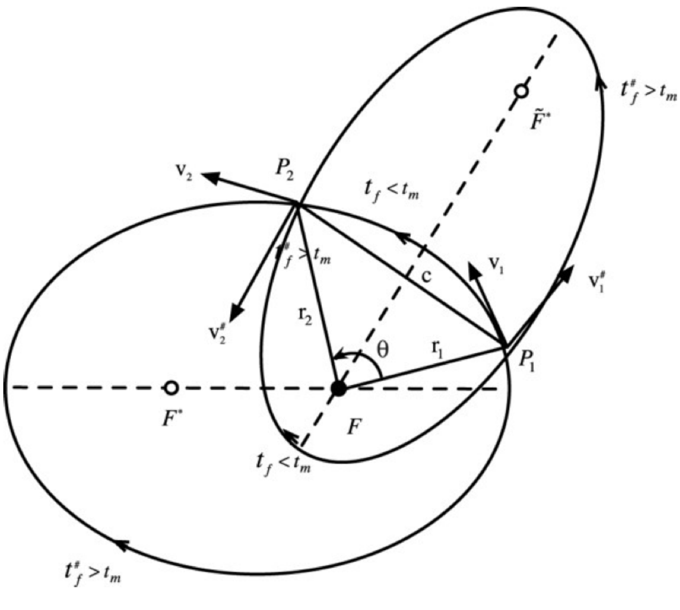

Figure 7: Parameters in Lambert's Theorem[16]

DOI: 10.13009/EUCASS2023-644

$$\sin(\frac{\alpha}{2}) = \sqrt{\frac{s}{2a}} \tag{38}$$

$$\sin(\frac{\beta}{2}) = \sqrt{\frac{s-r}{2a}} \tag{39}$$

$$s = \frac{r_1 + r_2 + c}{2} \tag{40}$$

$$c = ||\mathbf{r}_1 - \mathbf{r}_2|| \tag{41}$$

Then the initial and final maneuvers are obtained by[16]

$$\Delta\mathbf{v}_{L1} = \sqrt{\frac{\mu}{4a}}[(\cot(\frac{\alpha}{2} + \cot(\frac{\beta}{2}))\frac{\mathbf{r}}{c}) + (\cot(\frac{\beta}{2} - \cot(\frac{\alpha}{2}))\frac{\mathbf{r}_1}{||\mathbf{r}_1||})] \tag{42}$$

$$\Delta\mathbf{v}_{L2} = \sqrt{\frac{\mu}{4a}}[(\cot(\frac{\alpha}{2} + \cot(\frac{\beta}{2}))\frac{\mathbf{r}}{c}) - (\cot(\frac{\beta}{2} - \cot(\frac{\alpha}{2}))\frac{\mathbf{r}_2}{||\mathbf{r}_2||})] \tag{43}$$

In this study, we apply Lambert's theorem to determine the magnitude and direction of the maneuver from our A3 phasing orbit to the target point, after implementing the Δv_3 phasing orbit transition maneuver. This enables the satellite to transition from its original deviated trajectory to our target point, reducing the errors caused during the transition and allowing the satellite to reach its destination more precisely.

7. Numerical Simulaton

In the simulation, some of them are identical to the simulations in the 2BP model but some are not. We here list the different conditions:

7.1 Specifications of the Orbits

Parking Orbit:

- Mission duration:
  - Departure time: 07 Sep 2024 04:00:00.000 UTC, 60560 (MJD)
  - Arrival time: 10 Oct 2024 00:00:00.000 UTC, 60593 (MJD)
  - Mission duration: 33 days.
- Assumptions
  - Initial position of the spacecraft: Initial mean anomaly M = 30 (deg)
  - Environment: ER3BP

7.2 Initial Conditions

The Insertion points of the satellite in r_{SOI} in the Cartesian coordinate system in lunar-centered Inertial frame (LCI):

$$\mathbf{r}_{sc,SOI} = \begin{bmatrix} 65455.9204 & 18929.7464 & -579.1054 \end{bmatrix} \text{(km)} \tag{44}$$

$$\mathbf{v}_{sc,SOI} = \begin{bmatrix} -0.7993 & -0.2016 & 0.0762 \end{bmatrix} \text{(km/sec)} \tag{45}$$

The above parameters can be converted to the Cartesian coordinate system in earth-centered Inertial frame (ECI):

$$\mathbf{r}_{sc,SOI} = \begin{bmatrix} -4416.5352 & -322540.9474 & -178689.4935 \end{bmatrix} \text{(km)} \tag{46}$$

$$\mathbf{v}_{sc,SOI} = \begin{bmatrix} 0.1822 & -0.3608 & -0.0962 \end{bmatrix} \text{(km/sec)} \tag{47}$$

DOI: 10.13009/EUCASS2023-644

Table 3: Orbit elements of the parking and target orbit

	Parking orbit	Target
a	24628.1370 (km)	194053.8749 (km)
e	0.7207	0.9645
i	33.7582263933801 (deg)	33.7582 (deg)
Ω	-33.8670460776259 (deg)	-33.8670 (deg)
ω	121.864306664556 (deg)	121.8643 (deg)
f	118.6735 (deg)	0.0001 (deg)

After trial and error, it was finally found that applying a deceleration correction of 0.1171 km/s during the back-integration can make the back-integration close to the target perigee height when returning to Earth. The orbit elements of parking orbit and target orbit are provided in Tab. 3, where the target orbit is the one that back integrated from the insertion point.

After applying the algorithm, in the following list the result:

- Final state of the spacecraft in the LCI

$$\mathbf{r}_f = \begin{bmatrix} -1468.7794 & -528.4610 & 1235.6370 \end{bmatrix} \text{(km)} \tag{48}$$

$$\mathbf{v}_f = \begin{bmatrix} -1.5107 & -0.1738 & -1.7772 \end{bmatrix} \text{(km/sec)} \tag{49}$$

- Error between the final state and the insertion point.

$$\delta\mathbf{r} = \begin{bmatrix} 109.4318 & 164.2249 & -54.7719 \end{bmatrix} \text{(km)} \tag{50}$$

$$\delta\mathbf{v} = \begin{bmatrix} 0.0071 & -0.2291 & -0.0779 \end{bmatrix} \text{(km/sec)} \tag{51}$$

It is apparent that the error is very small relative to the whole mission. The results are also verified using STK under full perturbations. The complete maneuvers are listed in Table 4 The simulation result is shown in Fig. 8.

Table 4: Complete Manevbers

	Δv (km/s)	a_k (km)	T_k (sec)	n_k (cycle)	dN_k (cycle)	Δt (sec)
Parking	/	24628.137	38464.5537	14	0	204.629283120562
Phasing 1	0.300	39322.0129	77600.5359	13	-1	-127.057239503587
Phasing 2	0.0945	49172.0956	108514.8469	8	0	126.754433293555
Correction	Δv (km/s)	T_{TCM} (sec)				
Phasing 3	0.2913	14397.0912	0	/	/	/
TCM 1	0.0295	55067.9137	/	/	/	/
TCM 2	0.0045	10354.6383	/	/	/	/
TCM 3	0.0540	42932.4107	/	/	/	/
TCM 4	0.0066	11241.9019	/	/	/	/
TCM 5	0.0165	151039.501938066	/	/	/	/
TCM 6	0.0226	45658.7426934090	/	/	/	/
TCM 7	0.1239	69614.8047516166	/	/	/	/

8. Conclusion

This research designs a common phase loop transfer orbit design process for different Earth-Moon missions and different mission constraints. Through this design process, a series of phase loop transfer orbit parameters can be designed within a specified time, under limited resources and engineering constraints, so that the spacecraft can reach the target point under various constraints. As shown in the examples, the initial conditions in this study are different because this design process can be applied to arbitrary departure conditions. During the design process, the required parameters can be estimated under the two-body environment, and then different perturbations are considered, such as the J_2 effect of

DOI: 10.13009/EUCASS2023-644

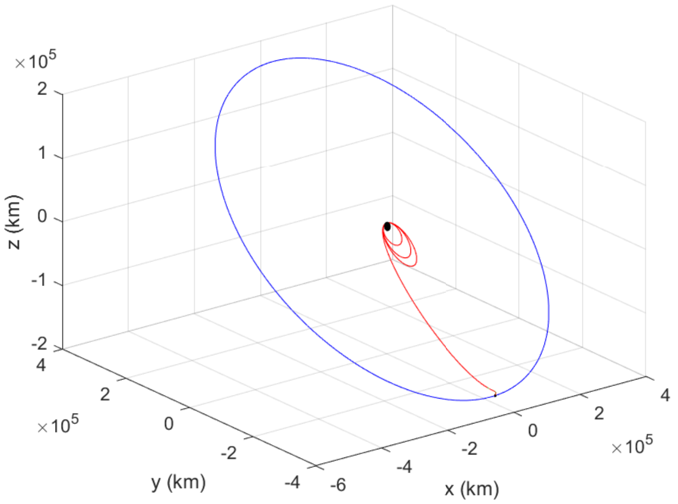

Figure 8: Simulated full transferring orbits

the Earth or the perturbation caused by the gravity of minor celestial bodies. If the spacecraft does not return to the perigee at a specific time, modify the time for the spacecraft to return to the perigee under the influence of perturbations to ensure that the maneuver is implemented at the perigee. The last half-cycle of the phase loop transfer orbit mainly uses Lambert's theorem to find out the impulsive correction maneuver to achieve orbit correction. The elliptic restricted three-body environment is also employed to simulate the A3 loop. Due to the introduction of lunar gravity, one or two more correction maneuvers can be used for more accurate results.Therefore, under this design process, the spacecraft only needs 5 correction maneuvers, and it can also make the spacecraft reach the destination with fewer errors. The Systems Tool Kit (STK) is also used to verify our design. The developed algorithm in this paper is potentially applicable to various lunar mission scenarios using phasing-loop transfer provided desired initial and terminal conditions.

9. Acknowledgments

The work described here is funded by the Taiwan Ministry of Science and Technology through project NSTC-111-2221-E-032 -011.

References

[1] C.-W. Wong and F.-Y. Hsiao. Design of Translunar Injection Trajectories Using Phasing Loop under ER3BP Environment. International Conference on Astronautics and Space Exploration (iCASE), November 2021.

[2] S.-J. Choi, Y.-J. Song, J. Bae, E. Kim, and G. Ju. Design and analysis of korean lunar orbiter mission using direct transfer trajectory. *Journal of the Korean Society for Aeronautical and Space Sciences*, 41:950–958, 2013.

[3] S.-J. Choi, I.-K. Kim, S.-M. Moon, C. Kim, and D. young Rew. A study on the analysis of visibility between a lunar orbiter and ground stations for trans-lunar trajectory and mission orbit. *Journal of the Korean Society for Aeronautical and Space Sciences*, 44:218–227, 2016.

[4] S.-J. Choi, D. Lee, I.-K. Kim, J.-W. Kwon, C.-H. Koo, S. Moon, C. Kim, S. Y. Min, and D.-Y. Rew. Trajectory optimization for a lunar orbiter using a pattern search method. *Proceedings of the Institution of Mechanical Engineers, Part G: Journal of Aerospace Engineering*, 231(7):1325–1337, 2017.

[5] S.-J. Choi, D. Lee, S.-B. Lim, and S.-W. Choi. Mission design and analysis based on sem angle by using variable coast during 3.5 earth-moon phasing loop transfer. *Journal of the Korean Society for Aeronautical and Space Sciences*, 46:68–77, 2018.

DOI: 10.13009/EUCASS2023-644

[6] S.-J. Choi, R. Whitley, G. Condon, M. Loucks, J.-i. Park, S.-W. Choi, and S.-J. Kwon. Trajectory design for the korea pathfinder lunar orbiter (kplo). *Proceedings of AAS/AIAA Astrodynamics Specialist Conference*, pages 1231–1244, 2018.

[7] D. Lee. Orbit transfer trajectory design using finite-burn maneuver under steering-angle constraints. *Proceedings of AAS/AIAA Astrodynamics Specialist Conference (AAS 17-835)*, 2017.

[8] D. Davis, J.-I. Park, S.-J. Choi, R. Whitley, J. Carrico, Y. Rew, and S.-W. Choi. Enhanced station-keeping maneuver control technique for delta-v cost reduction in korea pathfinder lunar orbiter. AAS/AIAA Astrodynamics Specialist Conference, August 2018.

[9] V. Szebehely and G. E. O. Giacaglia. On the elliptic restricted problem of three bodies. *Astronomical Journal*, 69:230, April 1964.

[10] A. Umar and A. A. Hussain. Motion in the er3bp with an oblate primary and a triaxial stellar companion. *Astrophysics and Space Science*, 361(10):344, September 2016.

[11] A. Hussain and U. Aishetu. Generalized out-of-plane equilibrium points in the frame of elliptic restricted three-body problem: Impact of oblate primary and luminous-triaxial secondary. *Advances in Astronomy*, 2019:1–12, February 2019.

[12] J. Miller. Lunar transfer trajectory design and the four body problem. 13th AAS/AIAA Space Flight Mechanics Meeting (AAS 17-835), February 2003.

[13] A. Kam, L. Plice, K. Galal, A. Hawkins, L. Policastri, M. Loucks, C. Nickel, R. Lebois, R. Sherman, and J. Carrico. Ladee flight dynamics: Overview of mission design and operations. 2015 AAS/AIAA Space Flight Mechanics Meeting, January 2015.

[14] Y. Qi and S. Xu. Minimum δv for the transfer to permanent lunar orbits with hyperbolic approach. *Acta Astronautica*, 119:183–195, 2016.

[15] C.-W. Wong. Design of translunar injection trajectories by using phasing loop. Master thesis, Department of Aerospace Engineering, Tamkang University, June 2022.

[16] D. Izzo. Revisiting lambert?s problem. celestial mechanics and dynamical astronomy. *Celestial Mechanics and Dynamical Astronomy*, 121(1):1–15, 2015.